AAPS PharmSciTech (2022) 23: 209
https://doi.org/10.1208/s12249-022-02367-w

RESEARCH ARTICLE

Advancements in Amorphous Solid Dispersions to Improve Bioavailability

Determination of Alteration in Micromeritic Properties of a Solid Dispersion: Brunauer-Emmett-Teller Based Adsorption and Other Structured Approaches

Lovepreet Singh[1] · Lakhvir Kaur[1] · Gurjeet Singh[1] · R. K. Dhawan[2] · Manjeet Kaur[1] · Navdeep Kaur[3] · Prabhpreet Singh[3]

Received: 24 December 2021 / Accepted: 11 July 2022 / Published online: 28 August 2022
© The Author(s), under exclusive licence to American Association of Pharmaceutical Scientists 2022

Abstract

The present study is focused on the use of solid dispersion technology to triumph over the solubility-related problems of bexarotene which is currently used for treating various types of cancer and has shown potential inhibitory action on COVID-19 main protease and human ACE2 receptors. It is based on comparison of green locust bean gum and synthetic poloxamer as polymers using extensive mechanistic methods to explore the mechanism behind solubility enhancement and to find suitable concentration of drug to polymer ratio to prepare porous 3rd generation solid dispersion. The prepared solid dispersions were characterized using different studies like X-ray diffraction (XRD), thermal gravimetric analysis (TGA), scanning electron microscopy (SEM), Brunauer-Emmett-Teller (BET), differential scanning calorimetry (DSC), and particle size analysis in order to determine the exact changes occurred in the product which are responsible for enhancing solubility profiles of an insoluble drug. The results showed different profiles for particle size, solubility, dissolution rate, porosity, BET, and Langmuir specific surface area of prepared solid dispersions by using different polymers. In addition to the comparison of polymers, the BET analysis deeply explored the changes occurred in all dispersions when the concentration of polymer was increased. The optimized solid dispersion prepared with MLBG using lyophilization technique showed reduced particle size of 745.7±4.4 nm, utmost solubility of 63.97%, pore size of 211.597 Å, BET and Langmuir specific surface area of 5.6413 m^2/g and 8.2757 m^2/g, respectively.

Keywords BET · Lyophilization · Solid dispersion · Dissolution enhancement · Locust bean gum

Introduction

Inadequate solubility of a therapeutically effective drug can hinder or even prevent drug development, yet the number of poorly soluble drugs is dramatically surging, leaving gaps in the development pipelines. Solubility also affects the optimization of the manufacturing process and reduces the effectiveness of the drug. Several approaches have been reported in the literature to amplify the solubility and bioavailability of poorly water-soluble drugs such as chemical modification, alteration of solvent composition, use of carrier system, and physical modification including solid dispersion method [1, 2]. Solid dispersion is one of the best alternatives to many other strategies in increasing solubility of poorly soluble drugs as it offers a variety of processing and excipient options that enhances the operational flexibility while formulating oral drug delivery systems [1–3]. Also, in solid dispersions, the poorly soluble drug sometimes gets transform into amorphous form in amorphous polymer matrix and possesses higher metastable energy state which leads to enhanced solubility and bioavailability of compound [4, 5]. Improvement in the wettability of the drug (which is improved by direct contact with the hydrophilic

✉ Lakhvir Kaur
lakhvir86@gmail.com

[1] Department of Pharmaceutics, Khalsa College of Pharmacy, Amritsar, Punjab 143001, India

[2] Department of Pharmacology, Khalsa College of Pharmacy, Amritsar, Punjab 143001, India

[3] Department of Chemistry, Guru Nanak Dev University, Amritsar, Punjab 143001, India

matrix), particle size reduction, increased surface area, and transformation from crystalline to amorphous state has been considered as the key mechanism for enhancing dissolution and bioavailability of any drug by formation of dispersions [6, 7].

In the last decade, the rate of occurrence of cancer has surged drastically and it has become the major cause of mortality around the world. Globally, the pervasiveness of malignancy has broadened; just in the USA, around 18,98,160 individuals endured cancer in 2021 [8]. Among anti-cancer drugs, Bexarotene (BEX) belongs to a retinoic acid family and is a profoundly selective and blood-brain barrier permeable RXR agonist [9]. It acts by inducing cell differentiation, apoptosis, and inhibiting metastasis [10]. Food and Drug Administration (FDA) approved BEX for treating cutaneous lymphoma [11–14]. BEX molecule was also found to be neuroprotective against myriad of neurological diseases, for instance, Alzheimer's disease, traumatic brain injury, and ischemic stroke [15–17]. Additionally, it shows promising inhibitory effect against non-small cell lung cancer (NSCLC), ER-negative breast cancer, and prostate cancer [18]. BEX has shown a synergistic effect with Docetaxel in Castrate-resistant prostate cancer inhibiting cyclinB1 and CDK1 expression levels [19]. Recently, this drug has also been found to be effective against COVID-19 virus (SARS-CoV-2) [20–22].

Due to poor fluid solvency of BEX, less proportion of drug gets absorbed following oral administration [23]. Hence, in order to improve the oral bioavailability of BEX, the current study is emphasized to prepare solid dispersion of this drug and to determine the mechanism behind the solubility enhancement effect resulted by formation of solid dispersions by Brunauer-Emmett-Teller (BET) surface area analysis, thermal gravimetric analysis (TGA), powder X-Ray diffraction study (XRD), differential scanning calorimetry (DSC), scanning electron microscopy (SEM), and particle size analysis studies.

Materials and Methods

Materials

Bexarotene was obtained as a gift sample from Apicore Pharmaceuticals Pvt. Ltd. Wilson Laboratories Mumbai, Maharashtra, supplied the locust bean gum polymer. Sigma Aldrich, Mumbai, Maharashtra, provided the poloxamer 188. Ethanol and methanol were purchased from S.D. Fine Chemicals, Mumbai. Dimethyl sulfoxide was purchased from Thermo Fisher Scientific Pvt. Ltd. Mumbai. Di-sodium hydrogen phosphate dihydrate and sodium dihydrogen orthophosphate dihydrate were purchased from Merck Life Science Pvt. Ltd. Mumbai and Hi-Media laboratories Pvt. Ltd. Mumbai, respectively. HPLC grade acetonitrile and methanol were purchased from Merck Life Science Pvt. Ltd. Mumbai. All other compounds were of analytical grade.

Modification of Locust Bean Gum Polymer

Before using Locust Been Gum (LBG) as a polymer, it was modified to improve its efficacy in solid dispersions to enhance the solubility of BEX. The method described by Murali *et al.* [24] was used to prepare modified locust bean gum (MLBG). In this method, the powdered LBG was first heated in a hot-air oven (Decibel, Chandigarh, India) at 120°C for 2 h. The prepared MLBG was then sieved (100 mesh) and stored in an airtight container at 25°C [5, 6]. The viscosity of both MLBG and LBG was determined by a viscometer. Swelling index, hydration capacity, moisture sorption capacity, angle of repose, and Carr's index of both polymers were also evaluated [5, 24].

Solubility Studies

In various solvents, solubility of BEX was determined. In 10 ml of each solvent, an excess quantity of BEX was added in screw-capped vials, and vials were then kept on a water bath shaker (NSW-125; Narang Scientific Works, New Delhi, India) at 37 ± 1°C for 48 h [3, 25]. The solutions were filtered through membrane filters (Millipore Corp., Billerica, MA, USA) of pore size 0.45 µm and analyzed by UV-VIS spectrophotometer (UV1900, Shimadzu).

Drug Excipient Compatibility Studies

The compatibility of the drug and polymer used within systems while designing solid dispersions should be determined. It is, therefore, necessary to confirm that under experimental conditions (40 ± 5°C and 75 ± 5% RH) for 3 months, the drug does not show any incompatibility with the polymer. The appropriate amount of drug was mixed separately with the polymers poloxamer 188 (POLO) and MLBG in a 1:5 ratio, sieved, and packed into dried vials. The vials were kept under above mentioned conditions and then examined at regular intervals to determine discoloration, clump formation, and liquefaction. In addition, FTIR spectra of drug, polymers, and physical mixtures were also recorded to analyze drug excipient compatibility [5].

Formulation Preparation

Lyophilization (Freeze-Drying Method)

The freeze-drying method was used to prepare the solid dispersion. Phase I was prepared by dissolving BEX in sufficient quantity of ethanol. Similarly, in phase II, polymers

were dissolved separately in water, and both phases were mixed separately with individual drug solutions. Ethanol was then evaporated, and the resulted solution was frozen in a deep freezer (RQFV-265; REMI Elektrotechnik, Mumbai, India) at −80°C and was then lyophilized in a freeze dryer (LyoQuest-55; Azbil Telstar Technologies, Terrassa, Spain) at a temperature of −40°C and a vacuum of 0.200 mbar. Then freeze-dried mass was sieved through sieve no. 60 and stored in a desiccator [5, 26].

High-Performance Liquid Chromatography Method

A validated HPLC method was used for quantitative analysis of BEX. In brief, used HPLC system was lined with SPD-20A/20AV UV spectrophotometric detector, LC-20AT solvent supply unit, a Lichrospher C_{18} (5 mm), 4.6x250 mm column (Shimadzu Corporation, Kyoto, Japan). The system was accelerated with an isocratic flow of acetonitrile and methanol (50:50 v/v) at 1 ml/min. A 15-µL sample was injected by autosampler and monitored at a wavelength of 260 nm. The calibration curve was linear and had a correlation coefficient ($R^2 > 0.9996$) for 0.25–16 µg/ml concentration range [27, 28].

Characterization of Solid Dispersion Formulation

Drug Content and Percentage Yield

The percentage yield of solid dispersion was calculated in order to determine the losses incurred during the lyophilization process. Drug content was then quantified from prepared solid dispersions by dissolving solid dispersions equivalent to 10 mg of BEX according to the yield in ethanol. To obtain the theoretical concentration of 10 µg/ml, it was then diluted. The solution was filtered through membrane filters, and drug concentration was analyzed using HPLC. According to the final weight of solid dispersions obtained, the percentage yield of each formulation was determined using the following Eq. (1) [7, 29].

$$\text{Percentage yield} = \frac{\text{Practical weight of solid dispersion}}{\text{Theoretical weight of solid dispersion}} \times 100 \quad (1)$$

Solubility of Prepared Solid Dispersions

The formulation equivalent to 20 mg of drug was added in screw-capped vials containing 10 ml of distilled water to quantify the solubility of prepared solid dispersions. Now, sealed vials were placed on an isothermal water bath shaker (NSW-125; Narang Scientific Works, New Delhi, India) at 37 ± 1°C for 48 h [30]. The samples were centrifuged, and the supernatant was filtered using a membrane filter (Millipore Corp., Billerica, MA, USA) of pore size 0.45 µm. It was then diluted with triple distilled water and analyzed using HPLC.

In Vitro Drug Release Study

The dissolution studies of BEX and prepared solid dispersions using MLBG and POLO (equivalent to 5 mg of BEX) were performed at 100 rpm using dissolution apparatus (DS 8000; LABINDA, Navi Mumbai, India) in a hemispherical bottomed dissolution vessel in 900 ml of distilled water at 37 ± 0.5°C using USP type II apparatus (paddle type). At appropriate time intervals, aliquots of 5 ml were withdrawn and replaced with fresh dissolution medium [4, 26]. The samples were filtered using a membrane filter of pore size 0.45 µm (Millipore Corp., Billerica, MA, USA) and quantified using HPLC.

Mechanistic Studies

Particle Size

The particle size of the solid dispersions was analyzed using a particle size analyzer. The samples were dispersed in triple distilled water, diluted, and subjected to particle size analyzer (Zetasizer Nano ZS Malvern Instrument Ltd., UK) to determine size at 25.0 ± 0.1°C. The polydispersity index was also characterized by this method, which measures uniformity in size distribution [31]. The analysis was done in triplicate.

Thermal Gravimetric Analysis

Thermal gravimetric analysis (TGA) can be used as determining factor for weight gain/loss of the samples due to different factors. Weight gain predicts the adsorption or oxidation, and weight loss predicts decomposition, desorption, dehydration, desolvation, or volatilization [32, 33]. For testing, 3 mg of sample was taken and analyzed in pierced aluminum pan at temperature range of 25 to 1000°C and a heating rate of 10°C/min using an automatic thermal gravimetric analyzer (HITACHI STA7200) [34].

Attenuated Total Reflection-Fourier-Transform Infrared Spectroscopy

The Fourier transform infrared (FT-IR) spectra of drug, POLO, MLBG, prepared solid dispersions, and their respective physical mixtures was recorded using FTIR spectrophotometer (Perkin Elmer 92035). In the frequency range of 4000 cm^{-1} to 400 cm^{-1}, the spectrum was captured at an average of 64 scans [35, 36].

Differential Scanning Calorimetry

The phase transition of BEX and solid dispersions was analyzed by differential scanning calorimetry (DSC) (HITACHI DSC7020) at temperature range of 30 to 300°C, operated at a heating rate of 10°C/min under nitrogen atmosphere with a flow rate of 40 ml/min. Accurately weighed sample (~1.5–2.0 mg) was placed in a sealed pin-holed aluminum pan and empty aluminum pan was used as a reference. The stability of the baseline was checked prior to each measurement [37, 38].

X-Ray Diffraction

X-ray diffraction was employed to confirm the nature of drug, carriers, and solid dispersions. A powder X-Ray diffractometer (Rigaku diffractometer) was employed to carry out XRD at an angle of 2θ ranging from 0° to 80° with scanning speed of 4°/min, step size of 0.02° and step time of 18.7 min using CuKα (λ = 1.54 Å) emission of radiation as an X-ray source. The apparatus was operated at a voltage of 40 kV and a current of 45 mA [39, 40]. A Ni filter was employed for the radiation, and data was collected using a flat holder in Bragg Brentano geometry.

Scanning Electron Microscopy

The surface morphology of drug, POLO, MLBG, and prepared solid dispersions was examined using a scanning electron microscope (SUPRA-55; Zeiss, Germany) with 20 µm aperture, operated at an accelerating voltage of 10 kV under reduced pressure [41]. The powder sample was sprinkled directly over the brass stub with double-sided adhesive tape. Further, the samples were coated with gold (approximately 5 nm) under vacuum for 100 s at 30 W, and the stubs were observed under SEM [42].

Brunauer-Emmett-Teller

In order to investigate surface area and porosity, prepared dispersions were subjected to Brunauer-Emmett-Teller (BET) analysis (Micromeritics ASAP 2020, USA). The sample was weighed and then degassed at 50°C for 200 min on degas port of ASAP 2020. After completion of degassing, the measurements were performed at 77 K. [43–45].

Stability Studies

To investigate the stability of prepared BEX-MLBG and BEX-POLO solid dispersions, samples were exposed to 40°C and 75% RH for 180 days. After the completion of this period, the dissolution studies of the stored samples were carried out. Moreover, the solid dispersion samples were analyzed by differential scanning calorimetry (DSC), and X-ray diffraction (XRD) studies to determine whether there was any kind of recrystallization of product. The findings were compared with results of freshly prepared solid dispersions [46, 47].

Statistical Analysis

The data is presented as the mean ± standard deviation of three sets of results. Analysis of variance (ANOVA) followed by Tukey's test (Sigma stat 3.5; STATCON) was used to examine the statistical difference between solubility and dissolution efficiency. Statistical significance was defined as a value of $p < 0.05$.

Results

Preparation of Modified Locust Bean Gum

To enhance the efficacy of LBG in improving the solubility of BEX, it was modified to reduce the viscosity without altering any other parameters. The viscosity of LBG and MLBG was measured at different shear rates to observe the difference, and the findings are showed in Table I. There is a significant difference in viscosity between LBG and MLBG at a shear rate of 40 s^{-1} with the value of 1255 ± 15 cps and 140.3 ± 1.6cps, respectively, which shows that the viscosity of the polymer decreased 9-fold as a result of modification.

Solubility Studies

Before the preparation of solid dispersions, the solubility of BEX was determined in different solvents and the results are shown in Table II, indicating very poor solubility of 0.00018± 0.0002 mg/ml in distilled water.

Table I Characterization of LBG and MLBG

Parameter	Shear rate (s^{-1})	LBG	MLBG
Viscosity (cps)	10	1898 ± 25	191 ±1.6
	20	1635 ± 17	170.2 ± 1.8
	30	1420 ± 19	155.6 ±1.5
	40	1255 ± 15	140.3 ± 1.6
Swelling index (%)		1480 ± 13	1311 ± 13
Hydration capacity		2.9 ± 0.04	2.95 ± 0.03
Moisture sorption capacity		7.1 ± 0.15	13.11 ± 0.23
Angle of repose		37.1 ± 0.7	36.9 ± .09
Carr's index (%)		21.9 ± 0.5	20.94 ± 0.7

Table II Solubility of BEX in Different Solvents

S.No.	Solvent system	Solubility (mg/ml) ± S.D	Reported value (mg/ml)	Reference
1.	Ethanol	8.83± 0.51	10	[48]
2.	Methanol	7.54± 0.82	-	
3.	DMSO	62.48± 1.31	65	[48]
4.	Distilled water	0.00018± 0.0002	0.00024	[27]
5.	Phosphate buffer pH 6.8	0.00016± 0.0002	0.00019	[27]

Preparation of Solid Dispersions

Solid dispersions were then prepared in different drug to-polymer ratios ranging from 1:1 to 1:5 using MLBG and POLO as the carrier. The composition of all prepared solid dispersions of BEX using the lyophilization method is given in Table III: Drug content of all the formulations was found to be in the range 96.1 ± 1.3 to 99.1 ± 1.1%.

Solubility of Solid Dispersions

The solubility of all the formulations was determined in distilled water, and the results are shown in Table III. As the drug-to-polymer ratio was increased, it was found that the drug solubility also increased significantly in a linear fashion, with no substantial difference observed after 1:4 for POLO and MLBG. However, when the ratio was increased, the percentage yield was decreased in case of dispersions prepared with POLO.

In Vitro Drug Release Study

The results of dissolution profiles of BEX, prepared solid dispersions (BEX-MLBG(1:1), BEX-MLBG(1:2), BEX-MLBG(1:3), BEX-MLBG(1:4), BEX-MLBG(1:5), BEX-POLO(1:1), BEX-POLO(1:2), BEX-POLO(1:3), BEX-POLO(1:4), and BEX-POLO(1:5)), are shown in Fig. 1a, b. In comparison to the solid dispersions, BEX has the lowest dissolution rate. With increasing amount of MLBG and POLO (with MLBG BEX-MLBG(1:1) < BEX-MLBG(1:2) < BEX-MLBG(1:3) < BEX-MLBG(1:4) < BEX-MLBG(1:5), ; with POLO BEX-POLO(1:1) < BEX-POLO(1:2) < BEX-POLO(1:3) < BEX-POLO(1:4) < BEX-POLO(1:5)), solid dispersions showed enhanced dissolution.

Mechanistic Studies

Particle Size

The particle size of solid dispersion of the drug-to-polymer ratio of 1:4, as shown in Table III, prepared using lyophilization process, was 515.2 ± 4.2 and 745.7 ± 4.4 nm for POLO and MLBG, respectively. In addition, different other experiments were also performed to support the results of these two optimized formulations developed with different polymers.

Table III Composition and Characterization of Prepared Solid Dispersion

Compositions			Characterization				
Polymer	Formulation code	Drug carrier ratio	% yield	% drug content	Particle size	Solubility mg/ml	PDI
	BEX	-	-	-	-	0.00018	-
	BEX-POLO1	1:1	92.5±0.8	96.1±1.3	825.0±7.1	0.00162	0.302±21.3
	BEX-POLO2	1:2	85.2±1.2	96.9±1.4	721.8±9.1	0.00206	0.401±18.9
POLO	BEX-POLO3	1:3	82.9±1.1	97.5±1.1	694.1±3.5	0.00272	0.376±11.1
	BEX-POLO4	1:4	79.5±0.9	98.4±1.0	515.2±4.2	0.00356	0.448±14.1
	BEX-POLO5	1:5	73.6±1.0	99.1±1.1	471.5±5.3	0.00361	0.396±10.8
	BEX-MLBG1	1:1	94.7±0.8	96.3±1.8	918.3±7.1	0.00153	0.089±8.8
	BEX-MLBG2	1:2	95.0±1.1	97.1±1.1	875.9±6.5	0.00211	0.115±11.0
MLBG	BEX-MLBG3	1:3	94.1±1.2	96.8±1.4	795.3±7,1	0.00284	0.101±10.9
	BEX-MLBG4	1:4	95.1±1.4	99.0±1.2	745.7±4.4	0.00340	0.042±15.9
	BEX-MLBG5	1:5	95.4±0.9	97.1±1.7	605.8±5.3	0.00344	0.095±11.8

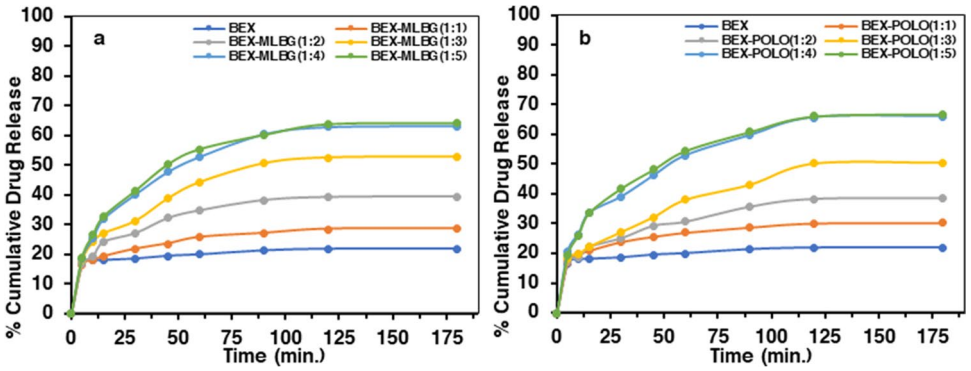

Fig. 1 **a** *In vitro* dissolution profile of BEX, solid dispersions of BEX with MLBG at 1:1(BEX-MLBG(1:1), 1:2(BEX-MLBG(1:2), 1:3(BEX-MLBG(1:3), 1:4(BEX MLBG(1:4), 1:5(BEX-MLBG(1:5). **b** *In vitro* dissolution profile of BEX, solid dispersions of BEX with POLO at 1:1(BEX-POLO(1:1), 1:2(BEX-POLO(1:2), 1:3(BEX-POLO(1:3), 1:4(BEX-POLO(1:4), 1:5(BEX-POLO(1:5)

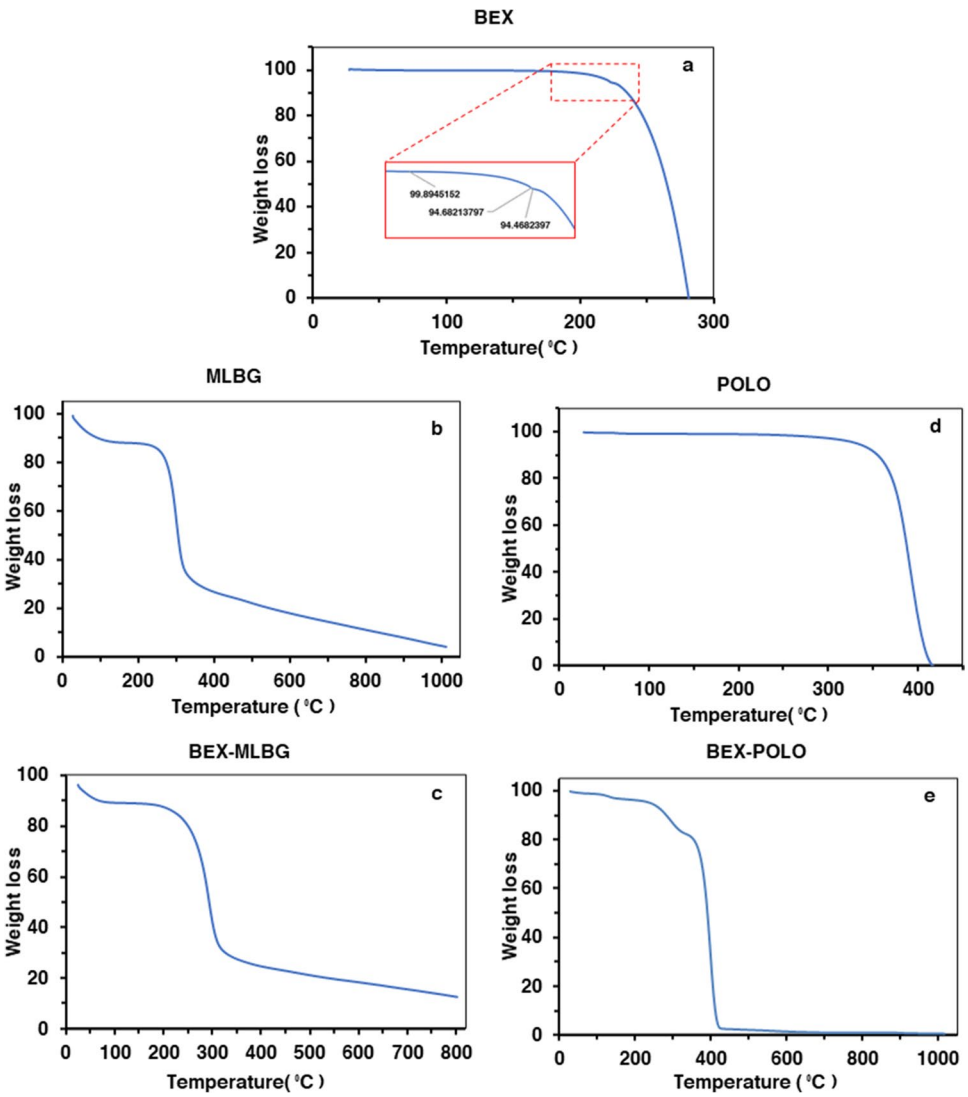

Fig. 2 TGA thermograms of **a** BEX, **b** MLBG, **c** BEX-MLBG, **d** POLO, and **e** BEX-POLO

TGA

The TGA thermogram of BEX (Fig. 2a) showed two mass loss events within temperature range of 161 to 223°C, with approximately 5.4% mass loss and within temperature range of 226 to 281.7°C, with almost 99% mass loss. MLBG (Fig. 2b) showed the total mass loss in three events. The first event occurred in the temperature range of 27.2 to 200.04°C, wherein the mass loss was 12.25%. The gradual mass loss occurred in the second event, within the temperature range of 210 to 322.12°C, wherein, the mass loss was around 64.34%. In the third event, the mass loss was slow, within the temperature range of 323 to 1012°C, approximately a mass loss of 98.2% occurred. In the thermogram of BEX-MLBG (Fig. 2c) solid dispersion, 10.8% mass loss took place in the first event within the temperature range of 27 to 100.9°C, 62.14% mass loss was observed in the second event within the temperature range of 248 to 305°C, and the third event occurred slowly within the temperature range of 305 to 803.20°C with approximately 88% mass loss. The TGA thermogram of POLO (Fig. 2d) exhibited a degradation process in the temperature range of 202 to 316.5°C, where the mass loss was approximately 4%, and in the temperature range of 327 to 414°C, about 98.9% mass loss was found. In the BEX-POLO (Fig. 2e) solid dispersion, within the temperature range of 47 to 151°C, 4% mass loss, and in the temperature range of 315.1 to 416°C, an approximately 94.65% mass loss occurred.

ATR-FTIR

The FTIR spectrum of pure BEX, POLO, MLBG, physical mixtures, and solid dispersions prepared with both polymers is shown in Fig. 3. Pure BEX FTIR spectra (Fig. 3a) exhibited characteristic peaks at 2922.2 cm $^{-1}$ for the C-H stretch of alkane, 2668.8 cm^{-1}, and 2542 cm^{-1} for O-H stretch of carboxylic acid, 1818 cm^{-1} for C=O stretch of anhydride, 1677.3 cm^{-1} for stretch of C=O, and 1425 cm^{-1} for C-O monomer. In the spectra of MLBG (Fig. 3b), characteristics peaks at 3324.8 cm^{-1} for O-H stretch, 2922 cm^{-1} for C-H stretch of alkane, 1640 cm^{-1} ring stretch of mannose and galactose, 1379 cm^{-1} for symmetrical stretch of -CH_2 and C-OH, and 1013 cm^{-1} for stretch of CH_2OH. In physical mixture of BEX-MLBG (Fig. 3c), the change in peaks was observed at 3213 cm^{-1} for O-H stretch, 2661 cm^{-1} and 2534 cm^{-1} for -OH stretch of carboxylic acid, 1826 cm^{-1} for C=O stretch of anhydride, 1669 cm^{-1} for C=O, 1610 cm^{-1} for ring stretch of mannose and galactose, and 1416 cm^{-1} for C-O stretch. The spectra of BEX-MLBG (Fig. 3d) solid dispersion showed change in wavelength at 3302 cm^{-1} for O-H stretch. Some peaks of BEX were superimposed by peaks of MLBG due to concentration factor. The spectra of POLO (Fig. 3e) exhibited characteristics peaks at 2877 cm^{-1} for stretch of aliphatic -CH, 1341 cm^{-1} for stretch of inplane -O-H, and 1095 cm^{-1} for stretch of C-O. In physical mixture (Fig. 3f) and solid dispersion (Fig. 3g) of BEX-POLO, the characteristics peaks of BEX and POLO were retained, which indicate the absence of interactions.

DSC

The DSC thermograms of BEX, polymers, physical mixture, and solid dispersions are shown in Fig. 4. The DSC thermogram of drug (a) showed a sharp melting endothermic peak at 225.9°C and enthalpy of fusion was 132 mJ/mg, which specifies its crystalline nature. The thermogram of MLBG (b) exhibited an endothermic peak at 93.2°C, the onset at 81.6°C, endset at 114.2°C, and enthalpy of fusion was 269 mJ/mg. The gap between onset and endset was 34°C, which indicate its amorphous nature. In thermogram of physical mixture of BEX and MLBG, the endothermic peaks of both compounds shifted to 223.8°C and 107.4°C, respectively. The MLBG endothermic peak shifted to higher temperature as well as onset and endset also shifted to 86.6°C and 147.8°C, respectively, even gap between onset and endset also increased. In the solid dispersion of BEX-MLBG, the endothermic peak of MLBG shifted more towards higher temperature than physical mixture at 115.4°C. As in thermogram of POLO, the endothermic peak was observed at 55°C and enthalpy was 138 mJ/mg. In physical mixture of BEX-POLO, the endothermic peak of BEX shifted towards lower temperature at 217°C and endothermic peak of POLO also shifted toward lower range at 54.3°C. In solid dispersion of BEX-POLO, endothermic peaks shifted more than its physical mixture as BEX endothermic peak shifted at 163.5°C and POLO endothermic peak shifted at 50.8°C and enthalpy also changed towards lower side.

X-Ray Diffraction

X-ray diffraction (XRD) diffractogram of pure drug, carriers, and solid dispersions is shown in Fig. 5. The XRD of pure BEX displayed highly intensive peaks at 2Θ values of 11.2^0, 12.3^0, 14.3^0, 18.4^0, and 22.98^0. In the diffractogram of POLO, two sharp peaks were observed at 2Θ values of 19^0 and 23.2^0, which indicate its crystalline nature. The high-intensity peaks of BEX diminished significantly in the case of solid dispersions prepared with POLO. However, in the case of solid dispersion prepared with MLBG, these characteristic peaks vanished, which suggested the suppression of drug's crystallinity by forming amorphous solid dispersions**.** The above results indicate the amorphization of BEX through the formation of solid dispersions, which significantly improve solubility.

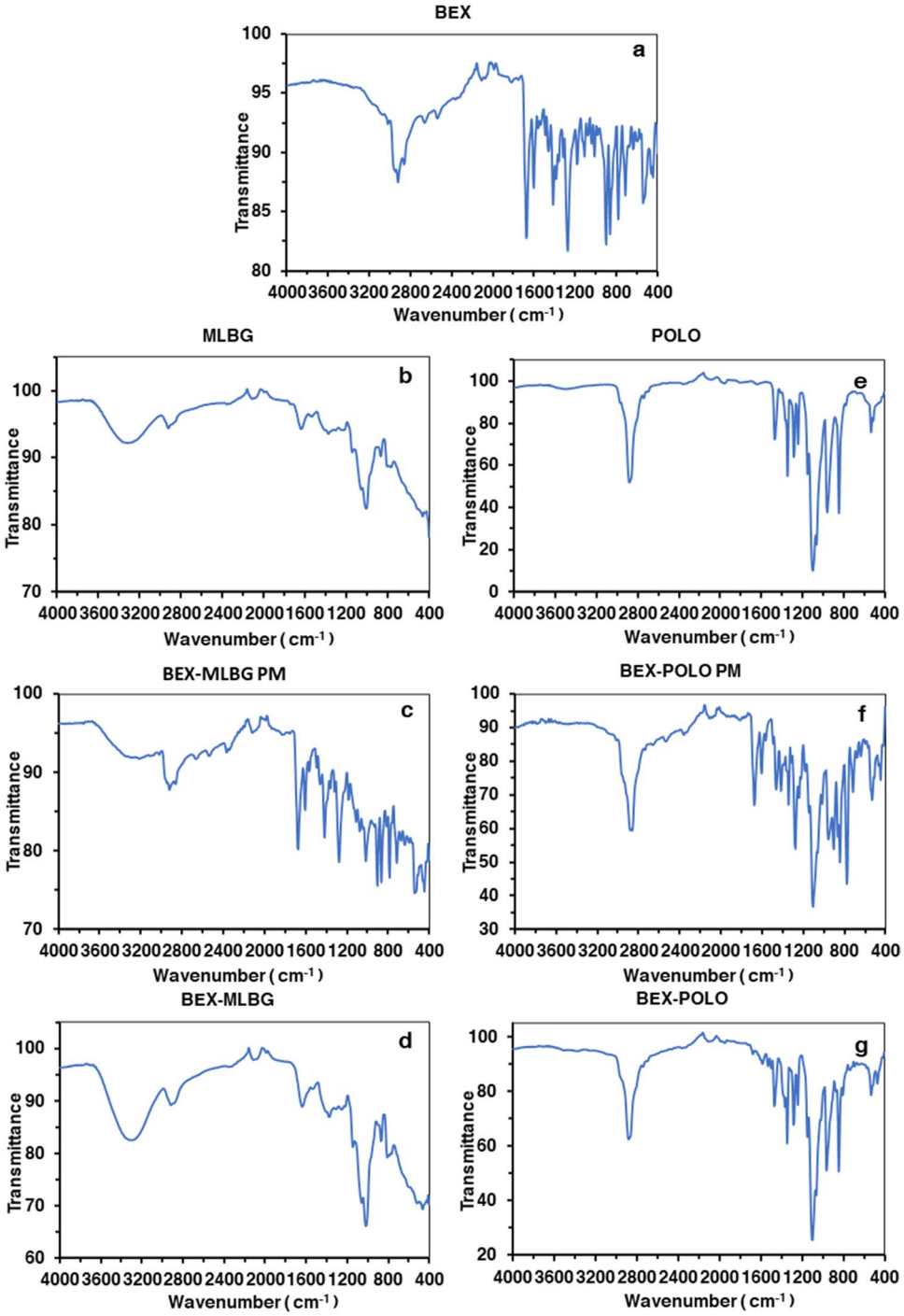

Fig. 3 FTIR spectrum of **a** BEX, **b** MLBG, **c** BEX-MLBG PM, **d** BEX-MLBG, **e** POLO, **f** BEX-POLO PM, and **g** BEX-POLO

SEM

The results of XRD were again verified with SEM studies. The micrograph of BEX reveals crystals with a rectangular shape predominance (Fig. 6a), correlating with the XRD data. The MLBG and POLO exhibited spherical surfaces (Fig. 6b, d). The image of BEX-MLBG (Fig. 6c) displayed an amorphous surface with no evidence of surface crystal. The image of formulation BEX-POLO (Fig. 6e) showed amorphous surface as compared to BEX-MLBG but seems less porous.

BET

BET analysis of drug and solid dispersion was carried out to analyze the porosity and specific surface area. This study uses the nitrogen gas adsorption/desorption isotherms method for analyzing the specific surface area, Langmuir

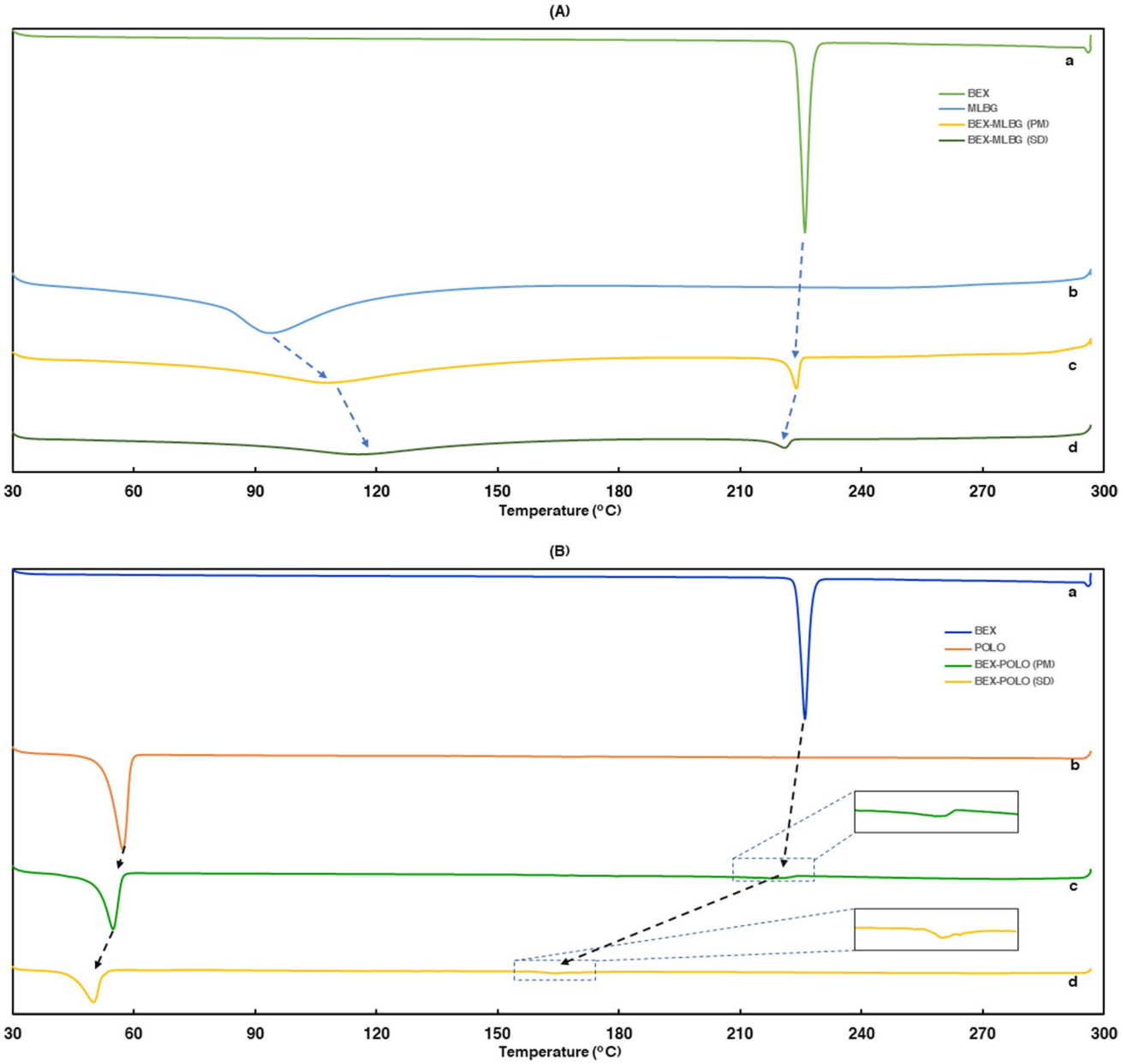

Fig. 4 **A** The DSC thermogram of (a) BEX, (b) MLBG, (c) BEX-MLBG (PM), and (d) BEX-MLBG (SD). **B** The thermogram of (a) BEX, (b) POLO, (c) BEX-POLO (PM), and (d) BEX-POLO (SD)

specific surface area, and porosity, and the observed spectra of solid dispersions and drug are shown in Fig. 7.

The quantity adsorbed was negative in both the isotherm linear and isotherm log absolute plots (Fig. 7), demonstrating that there was no gas adsorption with either BEX (Ia, Ib) or BEX-POLO (IIa, IIb), which indicates their impermeable characteristics. However, these plots were positive in the case of BEX-MLBG, showing a permeable or porous characteristics in increasing order with increase in drug-to-polymer ratio as shown in BEX-MLBG (1:3) (IIIa and IIIb), BEX-MLBG (1:4) (IVa and IVb), and BEX-MLBG (1:5) (Va and Vb). Furthermore, the BET specific surface area and Langmuir specific surface increased with increasing drug-to-polymer ratio. However, the pore size increased as the drug-to-polymer ratio was increased upto 1:4 and then sudden decrease was observed in 1:5, but the adsorption continued to increase as shown in Table IV.

Stability Studies

The dissolution profiles of optimized BEX-MLBG (AI) and BEX-POLO (AII) solid dispersions stored at

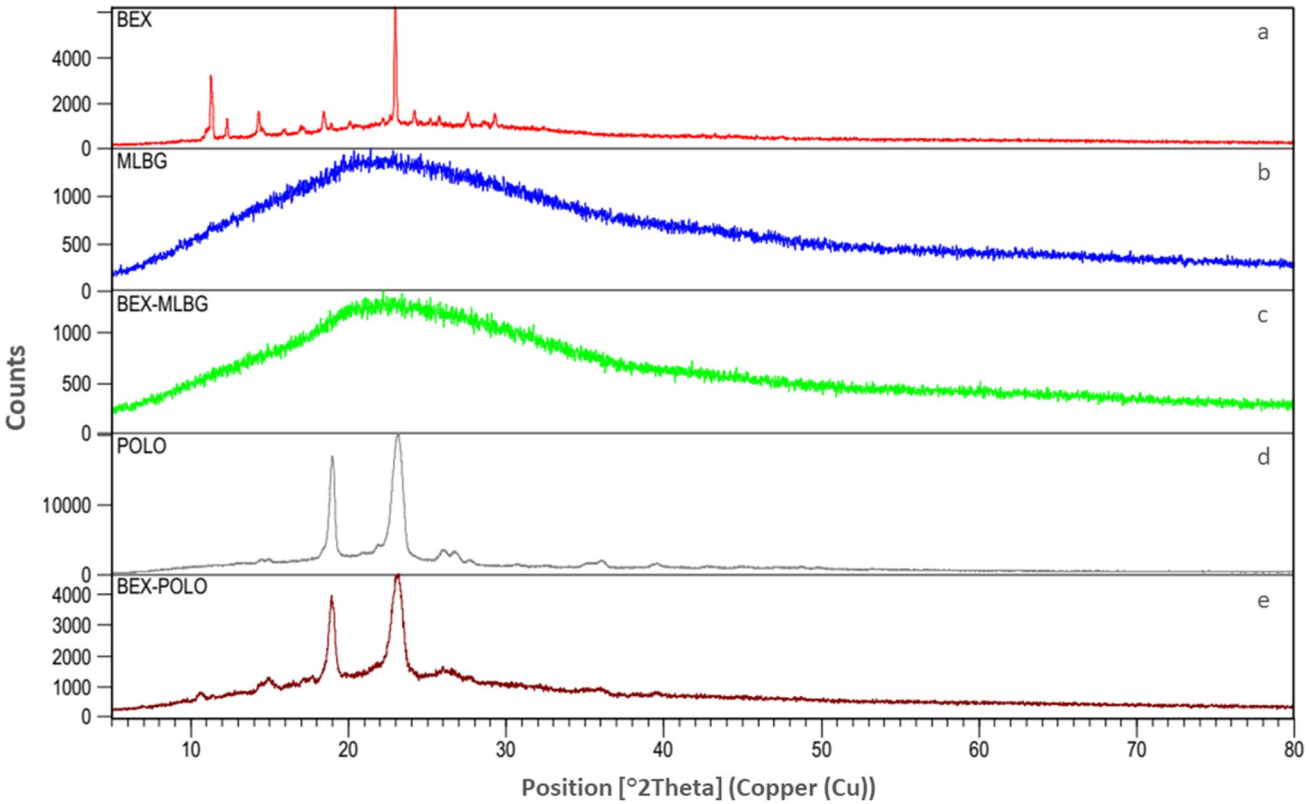

Fig. 5 The diffractogram of **a** BEX, **b** MLBG, **c** BEX-MLBG, **d** POLO, and **e** BEX-POLO

accelerated conditions for 180 days were found to be almost similar to freshly prepared solid dispersions, as shown in Fig. 8. In the DSC thermograms of solid dispersion BEX-MLBG (BII), the endothermic peaks of MLBG and BEX were observed at 115.4°C and 220.6°C, respectively, even after storage at accelerated conditions showing no significant difference in the endothermic peaks of freshly prepared solid dispersion (BI). Interestingly, in the BEX-POLO (BIV) solid dispersion, the crystallinity further diminished after storage, because the endothermic peaks of POLO and BEX were shifted toward lower temperature at 48.5°C and 160°C, respectively, which were 50.5°C for POLO and 163.5°C for BEX initially and also the enthalpy of fusion was almost half as compared to freshly prepared solid dispersion. Further, these findings were confirmed by the XRD study. In the diffractogram of BEX-MLBG (CII), no significant changes were observed after 180 days of storage at accelerated conditions. However, in the case of BEX-POLO solid dispersion, the intensity of peaks at 2Θ values of 19^0 and 23.2^0 significantly decreased to half when analyzed after 180 days as compared to fresh solid dispersions.

Discussion

The selection of a suitable polymer during the preparation of solid dispersions has considerable impact on the quality of final product. Due to this, solid dispersions were prepared using two polymers, wherein, LBG as green polymer and POLO as synthetic polymer were used to examine the effect of selection of a polymer on the solubility enhancement and overall impact on final formulation. As in the previous study reported by Singh *et al.* [5], the solid dispersion prepared by lyophilization possessed smaller size than that of other method. It is well established fact that smaller particles have large surface area to form contact with medium than that of larger particles, which results in higher dissolution rate [49]. Also, in a study by Singh *et al.* [5], solid dispersion with lyophilization technique showed better percentage release and dissolution efficiency than other techniques. This might be due to the formation of porous and fluffy products by the lyophilization technique, which increases the surface area and hence the surface free energy, resulting in increased solubility and dissolution [5, 6].

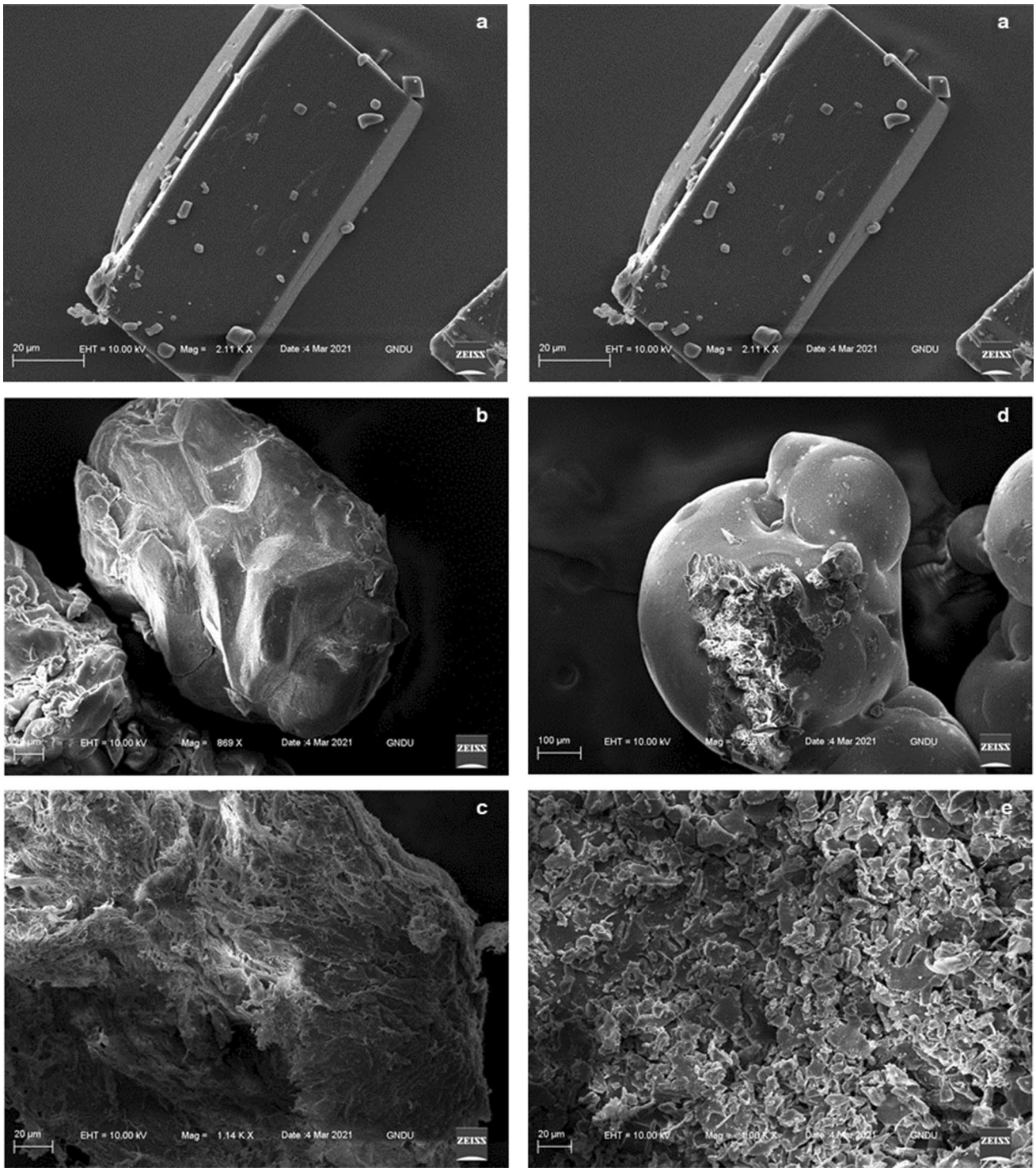

Fig. 6 Scanning electron microscope images of **a** BEX, **b** MLBG, **c** BEX-MLBG, **d** POLO, and **e** BEX-POLO

Hence, in order to investigate further and to determine the exact changes that occurred in the product by using same polymer and technique, we prepared the dispersions of another drug which possess anti-cancer activity and is recently reported to be effective against COVID-19 virus. LBG used as a green carrier showed different viscosity profiles before and after modification with a value of 1255 ± 15 and 140.3 ± 1.6 cps, respectively, due to its different chemical moieties interactions. This may be due to the reason that it is a neutral polysaccharide comprised of

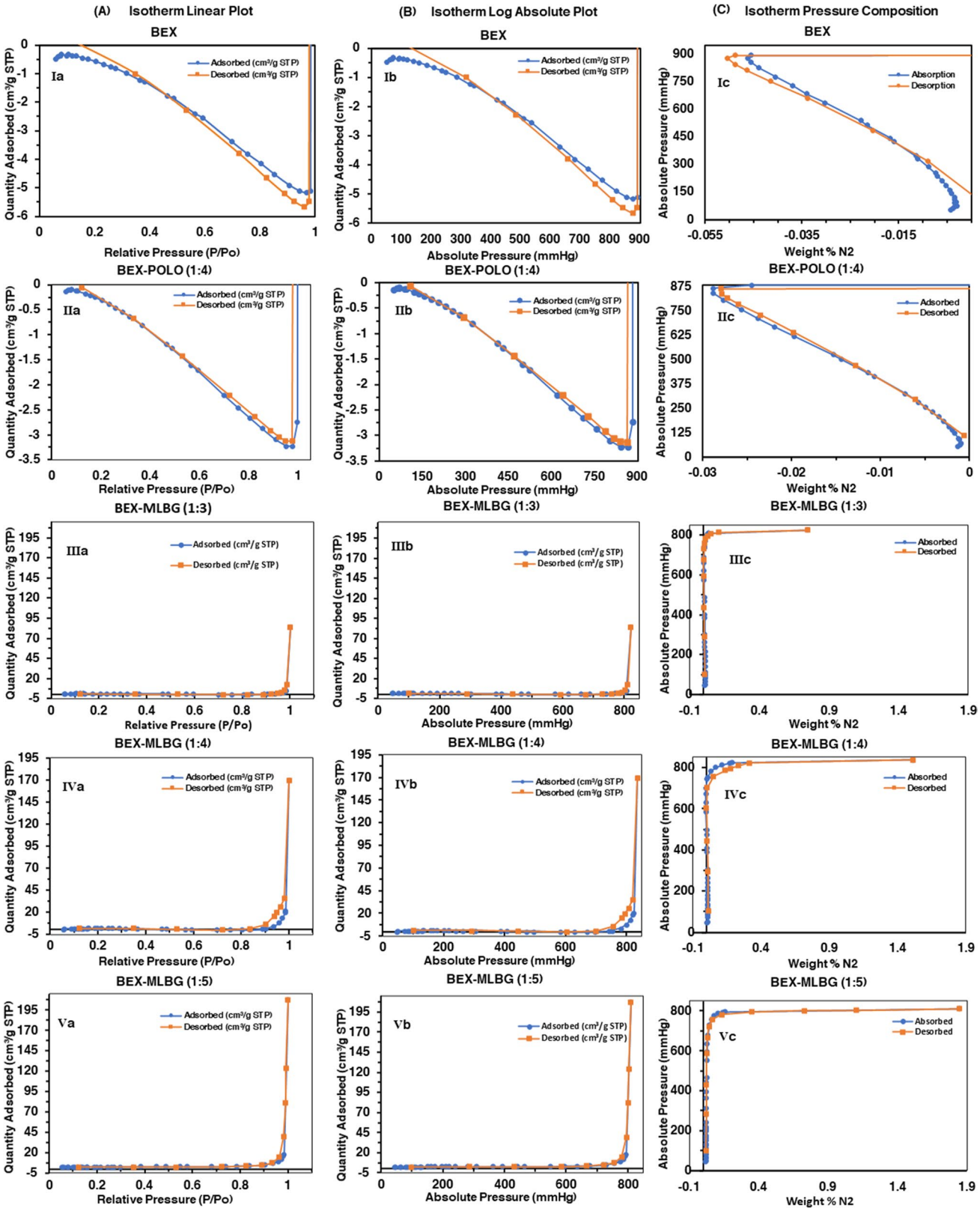

Fig. 7 **A** The isotherm linear plot between quantity adsorbed *vs*. relative pressure, (Ia) BEX, (IIa) BEX-POLO (1:4), (IIIa) BEX-MLBG (1:3), (IVa) BEX-MLBG (1:4), (Va) BEX-MLBG (1:5). **B** The isotherm log absolute plot between quantity absorbed *vs*. absolute pressure, portrays (Ib) BEX, (IIb) BEX-POLO (1:4), (IIIb) BEX-MLBG (1:3), (IVb) BEX-MLBG (1:4), (Vb) BEX-MLBG (1:5). **C** The isotherm pressure composition between absolute pressure *vs*. weight % N_2, portrays (Ic) BEX, (IIc) BEX-POLO (1:4), (IIIc) BEX-MLBG (1:3), (IVc) BEX-MLBG (1:4), (Vc) BEX-MLBG (1:5)

Table IV BET Specific Surface area, Langmuir Specific Surface Area and Pore Size

Samples	BET specific surface area (m^2/g)	Langmuir specific surface area (m^2/g)	Pore size (Å)
BEX	_____	_____	_____
BEX-POLO	_____	_____	_____
BEX-MLBG (1:3)	3.4528	4.4968	65.882
BEX-MLBG (1:4)	5.6413	8.2757	211.597
BEX-MLBG (1:5)	8.1954	10.9539	116.660

mannose and galactose units and hence classified under the category of galactomannans [50] and chemically it consists of (1-4)-linked β-D-mannose backbone and (1-6)-linked α-D-galactose side chains [50–52]. The mannose to galactose ratio for gums varies depending on the source, although values stated for LBG are normally in the range of 3.2–4.0 [53–55]. The side chain of galactose tends to impede molecular interactions and hence change in galactose lead to differences in functional characteristics of LBG, for example, solubility, viscosity, and gelation. LBG has a random and ordered blockwise distribution of galactose [55]. It is considered that interactions occurring between the unsubstituted smooth mannan sequences due to its numerous -OH groups make "hyperentanglements," which leads LBG to deviate from the usual concentration-dependent viscosity, resulting in higher viscosity at lower concentrations than many other galactomannans [56, 57]. This functionality of LBG was decreased by depolymerization on gentle heating [5, 24]. Additionally, LBG has a higher activation energy for degradation than other galactomannans, which is assumed to be related to its greater ability to interact in solution [58].

The physical mixtures of drug with both the polymers (POLO and MLBG) showed no sign of discoloration, clump formation, and liquefication for a period of 3 months. Then, the solid dispersions were prepared and characterized for different parameters to analyze the basic mechanism for enhancing solubility of a drug. In case of solid dispersions prepared with MLBG, as the drug-to-polymer ratio was increased, the solubility improved significantly. Moreover, with increase in drug-to-polymer ratio, the porosity increases, which further increases the surface area and hence increases the solubility by capillary and other mechanisms [49]. Furthermore, increasing the drug-to-polymer ratio after 1:4, there was no significant difference observed in solubility and *in vitro* dissolution profiles.

In case of solid dispersions prepared with POLO, the percentage yield decreased as the drug-to-polymer ratio increased and there was no significant increase in solubility after 1:4. This decrease in % yield was observed due to polymer which is sticky in nature [5]. Hence, drug-to-polymer ratio of 1:4 was shown to be optimal. In the case of solid dispersions made with MLBG, this effect of polymer on percentage yield was not observed, but there was significant enhancement in solubility. So, to compare the polymers at same ratios, we optimized drug:polymer ratio of 1:4 [5].

Then, the dissolution studies of all the formulations were carried out. It was observed that with increasing amount of MLBG and POLO, solid dispersions showed enhanced dissolution. The optimized dispersions were then characterized further to verify the results of solubility and dissolution studies. In TGA analysis, it was observed that the solid dispersions prepared with MLBG polymer showed minor fluctuations in mass loss, indicating increased thermal stability of dispersion at higher temperature when the percentage of mass loss were compared among both optimized dispersions, which might be due to interactions. TGA thermograms of BEX-polymer systems, indicated that the presence of BEX has minimal effect on the thermal profile of the polymeric carriers, a characteristic that strongly implies a favorable interface between drug and polymers [59–61].

Furthermore, the ATR-FTIR investigation was carried out which showed the changes in peaks wavelength in physical mixtures and solid dispersions which indicates the interactions between drug and polymers. The major change occurred in peak of BEX-MLBG solid dispersion at wavelength of 3302 cm^{-1} for -OH stretch which might be due to inter and intramolecular hydrogen bonding of MLBG [35, 62, 63]. However, in the case of BEX-POLO solid dispersion, no key changes were observed [50].

In DSC thermograms of solid dispersions, a little shift in the endothermic peak of the drug with lower intensity revealed that the drug had changed from crystalline to an amorphous state [5, 23, 38, 64, 65]. Further XRD study also confirmed the transformation of the crystalline drug into an amorphous form in solid dispersion. As in XRD pattern, BEX showed sharp peak at 2Θ values of 11.2^0, 12.3^0, 14.3^0, 18.4^0, and 22.98^0 indicating the crystalline nature of BEX [66]. MLBG diffractogram showed no sharp peak which indicates its amorphous nature. In case of solid dispersion prepared by MLBG, also there was no sharp peak, which indicates the amorphous nature of solid dispersion. Transformation of a crystalline state into an amorphous state results in enhancement of solubility [6]. In case of POLO, two sharp peaks were observed at 2Θ values of 19^0 and 23.2^0, which revealed its crystalline nature. The solid dispersion BEX-POLO diffractogram also displayed two peaks at 2Θ values of 19^0 and 23.2^0, but the peak of BEX was not observed [67, 68]. Moreover, these two peaks have less intensity than those of POLO, which demonstrate decrease in the crystallinity of the system. To further investigate, SEM was carried out, which supports the XRD results as BEX displayed crystals

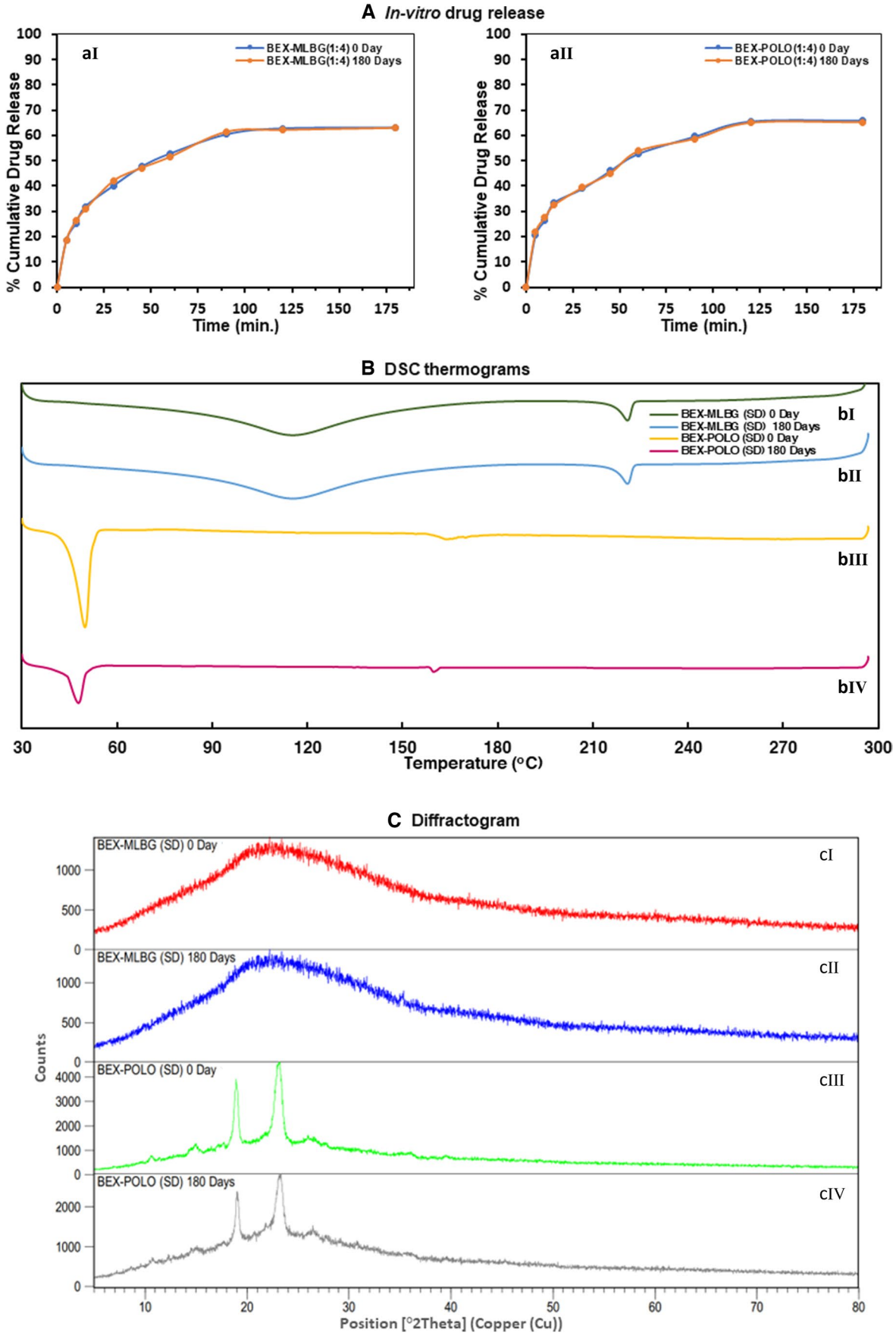
A In-vitro drug release
aI
BEX-MLBG(1:4) 0 Day
BEX-MLBG(1:4) 180 Days
% Cumulative Drug Release
Time (min.)
aII
BEX-POLO(1:4) 0 Day
BEX-POLO(1:4) 180 Days
% Cumulative Drug Release
Time (min.)
B DSC thermograms
BEX-MLBG (SD) 0 Day
BEX-MLBG (SD) 180 Days
BEX-POLO (SD) 0 Day
BEX-POLO (SD) 180 Days
bI
bII
bIII
bIV
Temperature (°C)
C Diffractogram
BEX-MLBG (SD) 0 Day
cI
BEX-MLBG (SD) 180 Days
cII
BEX-POLO (SD) 0 Day
cIII
BEX-POLO (SD) 180 Days
cIV
Counts
Position [°2Theta] (Copper (Cu))

◂**Fig. 8** **A** *In vitro* drug release profile of optimized solid dispersion on 0 day and after 180 days (AI) BEX-MLBG, (AII) BEX-POLO. **B** DSC thermograms of optimized solid dispersion (BI) BEX-MLBG on 0 day, (BII) BEX-MLBG after 180 days, (BIII) BEX-POLO on 0 day, (BIV) BEX-POLO after 180 days. **C** Diffractogram of optimized solid dispersion (CI) BEX-MLBG on 0 day, (CII) BEX-MLBG after 180 days, (CIII) BEX-POLO on 0 day, (CIV) BEX-POLO after 180 days

with a rectangular shape predominance [18]. Micrographs of MLBG and POLO revealed their spherical surfaces. The images of solid dispersion prepared using MLBG showed an amorphous surface and formation of a fluffy and porous matrix, while in the case of BEX-POLO, the solid dispersion is less porous. Porosity increases the solubility and dissolution by capillary mechanism. When it comes to drug loading and *in vitro* dissolution release, pore size and volume have a greater impact than surface area [69].

These results were further determined using BET analysis. In the case of solid dispersion of BEX-MLBG, as the drug-to-polymer ratio increased, the adsorption in the isotherm linear plot as well as isotherm log absolute increased, which indicates its permeable characteristic. Moreover, as drug-to-polymer ratio was increased, pore size also increased, which results in high specific surface area, and hence solubility and drug release increased. But in case of BEX-MLBG (1:5), no significant changes observed in drug release profiles [70]. Furthermore, as the drug-to-polymer ratio increased, the pore size increased linearly, but the results were contradicting in BEX-MLBG (1:5) as its pore size values were lower than BEX-MLBG (1:4) [71]. However, in case of BEX-MLBG (1:5), the adsorption, BET specific surface area, and Langmuir specific surface area values were higher than BEX-MLBG (1:3) and BEX-MLBG (1:4). The BET analysis results showed that the solid dispersion BEX-MLBG (1:5) has smaller pore size but high specific surface area, which indicate that pores population might have increased due to increase in polymer concentration which would have increased specific surface area. So, it predicts that, changes in pore size/pore population (as in the case of BEX-MLBG (1:5)) play a key role on the overall release kinetic and behavior of solid dispersions [69]. It can be inferred from the results of BET analysis that solid dispersion with drug to polymer ratio of 1:4 or above can be a good candidate for 3rd generation solid dispersions. Moreover, amorphous and porous solid dispersions are good candidates for 3D tablet printing [72, 73].

Then, the stability of prepared solid dispersions was determined under accelerated conditions for 180 days. The dissolution profile was found to be almost similar after storage. Moreover, the DSC thermograms of solid dispersion BEX-MLBG (BII) displayed no evidence of recrystallization. But in the case of BEX-POLO (BIV), the endothermic peaks were shifted towards the lower temperature and the enthalpy of fusion also decreased, which might indicate the further reduction in crystallinity upon storage. Further, these findings were confirmed by the XRD study; no changes were observed in the diffractogram of BEX-MLBG solid dispersion. However, the polymer peaks were less intense after storage period of 6 months in the case of BEX-POLO, which suggests that the crystallinity of the polymer was decreased and the findings are in accordance with the literature, where POLO has been proved to avoid retrogradation after storage [46, 47, 74].

Conclusion

It can be concluded from the above findings that the type of carrier has a considerable impact on the overall release kinetics of solid dispersions. Different parameters used to characterize prepared dispersions indicated that the crystallinity of product was reduced. BET analysis proved that the solid dispersion with drug to polymer ratio 1:4 or above can be a suitable candidate for 3rd generation solid dispersions. Also, BEX is reported to show dose-dependent response and is well tolerated drug which is also used in combination with other drugs to treat various diseases. Hence, for better patient compliance, BEX-MLBG combined solid dispersion at drug: polymer ratio of 1:4 or above could be potential candidate for 3D tablet printing for personalized medicine purposes.

Acknowledgements The authors gratefully acknowledge the support provided by Apicore Pharmaceutical Pvt. Ltd., India.

Author Contribution Research work idea by Gurjeet Singh, Lakhvir Kaur, and Lovepreet Singh. Data curation by Lovepreet Singh, Manjeet Kaur, and Navdeep Kaur. Formal analysis by Lovepreet Singh, Navdeep Kaur, Lakhvir Kaur, and Manjeet Kaur. Investigation by Lovepreet Singh and Navdeep Kaur. Methodology by Lakhvir Kaur, Lovepreet Singh, and Navdeep Kaur. Software by Gurjeet Singh and Lovepreet Singh. Supervision by Lakhvir Kaur, Gurjeet Singh, Prabhpreet Singh, and R.K. Dhawan. Validation by Lovepreet Singh, Gurjeet Singh, and Prabhpreet Singh. Visualization by Lakhvir Kaur and Gurjeet Singh. Writing Original Draft by Lovepreet Singh, Manjeet Kaur, and Navdeep Kaur. Writing review & editing by Lakhvir Kaur and Lovepreet Singh.

Declarations

Conflict of Interest The authors declare no competing interests.

References

1. Singh G, Kaur L, Gupta GD, Sharma S. Enhancement of the solubility of poorly water soluble drugs through solid dispersion: a comprehensive review. Indian J Pharm Sci [Internet]. 2017;79(5):674–87 Available from: www.ijpsonline.com.

2. Maulvi FA, Dalwadi SJ, Thakkar VT, Soni TG, Gohel MC, Gandhi TR. Improvement of dissolution rate of aceclofenac by solid dispersion technique. Powder Technol. 2011;207(1–3):47–54.
3. Oliveira V da S, Dantas ED, Queiroz AT de S, Oliveira JW de F, da Silva M de S, Ferreira PG, et al. Novel solid dispersions of naphthoquinone using different polymers for improvement of antichagasic activity. Pharmaceutics. 2020;12(12):1–15.
4. Wang X, Zhang L, Ma D, Tang X, Zhang Y, Yin T, et al. Characterizing and exploring the differences in dissolution and stability between crystalline solid dispersion and amorphous solid dispersion. AAPS PharmSciTech. 2020;21(7).
5. Singh G, Sharma S, Gupta G das. Extensive diminution of particle size and amorphization of a crystalline drug attained by eminent technology of solid dispersion: A comparative study. AAPS PharmSciTech 2017;18(5):1770–1784.
6. Gurjeet S, GDas G, Shailesh S. Effect of polymer and method on particle size and crystallinity of olmesartan medoxomil during the formulation of solid dispersion. Acta Pol Pharm Drug Res. 2017;74(5):1543–61.
7. Ganesan P, Soundararajan R, Shanmugam U, Ramu V. Development, characterization and solubility enhancement of comparative dissolution study of second generation of solid dispersions and microspheres for poorly water soluble drug. Asian J Pharm Sci. 2015;10(5):433–41.
8. Siegel RL, Miller KD, Fuchs HE, Jemal A. Cancer statistics, 2021. CA Cancer J Clin. 2021;71(1):7–33.
9. Dalal M, Mitchell S, McCloskey C, Zagadailov E, Gautam A. The clinical and humanistic burden of cutaneous T-cell lymphomas and response to conventional and novel therapies: results of a systematic review. Expert Rev Hematol. 2020;13(4):405–19.
10. Nosova YN, Zenin I v., Maximova VP, Zhidkova EM, Kirsanov KI, Lesovaya EA, et al. Influence of the number of axial bexarotene ligands on the cytotoxicity of Pt(IV) analogs of oxaliplatin. Bioinorg Chem Appl 2017;2017:1–6.
11. Tanita K, Fujimura T, Sato Y, Lyu C, Kambayashi Y, Ogata D, et al. Bexarotene reduces production of CCL22 from tumor-associated macrophages in cutaneous T-cell lymphoma. Front Oncol. 2019;9:1–10.
12. Beynon T, Selman L, Radcliffe E, Whittaker S, Child F, Orlowska D, et al. We had to change to single beds because i itch in the night: a qualitative study of the experiences, attitudes and approaches to coping of patients with cutaneous T-cell lymphoma. Br J Dermatol. 2015;173(1):83–92.
13. Denis D, Beneton N, Laribi K, Maillard H. Management of mycosis fungoides-type cutaneous T-cell lymphoma (MF-CTCL): focus on chlormethine gel. Cancer Manag Res. 2019;11:2241–51.
14. Zuo Y, Huang L, Enkhjargal B, Xu W, Umut O, Travis ZD, et al. Activation of retinoid X receptor by bexarotene attenuates neuroinflammation via PPARγ/SIRT6/FoxO3a pathway after subarachnoid hemorrhage in rats. J Neuroinflammation. 2019;21:16(1).
15. Cramer PE, Cirrito JR, Wesson DW, Lee CYD, Karlo JC, Zinn AE, et al. ApoE-directed therapeutics rapidly clear b-amyloid and reverse deficits in AD mouse models [Internet]. 2012. Available from: www.sciencemag.org
16. Dheer Y, Chitranshi N, Gupta V, Abbasi M, Mirzaei M, You Y, et al. Bexarotene modulates retinoid-X-receptor expression and Is protective against neurotoxic endoplasmic reticulum stress response and apoptotic pathway activation. Mol Neurobiol. 2018;55(12):9043–56.
17. Zhong J, Cheng C, Liu H, Huang Z, Wu Y, Teng Z, et al. Bexarotene protects against traumatic brain injury in mice partially through apolipoprotein E. Neuroscience. 2017;343:434–48.
18. Li L, Liu Y, Wang J, Chen L, Zhang W, Yan X. Preparation, in vitro and in vivo evaluation of bexarotene nanocrystals with surface modification by folate-chitosan conjugates. Drug Deliv. 2016;23(1):79–87.
19. Shen D, Wang H, Zheng Q, Cheng S, Xu L, Wang M, et al. Synergistic effect of a retinoid X receptor-selective ligand bexarotene and docetaxel in prostate cancer. OncoTargets Ther. 2019;12:7877–86.
20. Shahabadi N, Zendehcheshm S, Mahdavi M, Khademi F. Inhibitory activity of FDA-approved drugs cetilistat, abiraterone, diiodohydroxyquinoline, bexarotene, remdesivir, and hydroxychloroquine on COVID-19 main protease and human ACE2 receptor: a comparative in silico approach. Inform Med Unlocked. 2021;26:1–9.
21. Yuan S, Chan JFW, Chik KKH, Chan CCY, Tsang JOL, Liang R, et al. Discovery of the FDA-approved drugs bexarotene, cetilistat, diiodohydroxyquinoline, and abiraterone as potential COVID-19 treatments with a robust two-tier screening system. Pharmacol Res. 2020;1:159.
22. Tang B, Zhu J, Cong Y, Yang W, Kong C, Chen W, et al. The landscape of coronavirus disease 2019 (COVID-19) and integrated analysis SARS-CoV-2 receptors and potential inhibitors in lung adenocarcinoma patients. Front Cell Dev Biol. 2020;23:8.
23. Chen L, Wang Y, Zhang J, Hao L, Guo H, Lou H, et al. Bexarotene nanocrystal - oral and parenteral formulation development, characterization and pharmacokinetic evaluation. Eur J Pharm Biopharm. 2014;87(1):160–9.
24. Murali Gv, Babu M, Prasad CDS, Ramana Murthy K v. Evaluation of modified gum karaya as carrier for the dissolution enhancement of poorly water-soluble drug nimodipine. Int J Pharm [Internet]. 2002;234:1–17. Available from: www.elsevier.com/locate/ijpharm
25. Eedara BB, Nyavanandi D, Narala S, Veerareddy PR, Bandari S. Improved dissolution rate and intestinal absorption of fexofenadine hydrochloride by the preparation of solid dispersions: in vitro and in situ evaluation. Pharmaceutics. 2021;13(3):1–15.
26. Mudie DM, Stewart AM, Rosales JA, Adam MS, Morgen MM, Vodak DT. In vitro-in silico tools for streamlined development of acalabrutinib amorphous solid dispersion tablets. Pharmaceutics. 2021;1:13(8).
27. Ren S, Jiao L, Yang S, Zhang L, Song J, Yu H, et al. A novel co-crystal of bexarotene and ligustrazine improves pharmacokinetics and tissue distribution of bexarotene in SD rats. Pharmaceutics. 2020;12(10):1–20.
28. Venkata SRD, Raghuram P, Harikrishna KA. Development and validation of a novel stability indicating UPLC method for dissolution analysis of bexarotene capsules: an anti cancer drug. J Chromatogr Sep Tech. 2017;08(02).
29. Enose AA, Dasan PK, Sivaramakrishnan H, Shah SM. Formulation and characterization of solid dispersion prepared by hot melt mixing: a fast screening approach for polymer selection. J Pharm. 2014;2014:1–13.
30. Campos SN, Cid AG, Romero AI, Villegas M, Briones Nieva CA, Gonzo EE, et al. Solid dispersions as a technological strategy to improve the bio-performance of antiparasitic drugs with limited solubility. Proc West Mark Ed Assoc Conf. 2020;78(1):13.
31. Singh P, Kaur N. Cost-effective diagnostic kits for selective detection of gaseous H2S. New J Chem. 2021;45(36):16784–93.
32. Obaidat RM, Khanfar M, Ghanma R. A comparative solubility enhancement study of cefixime trihydrate using different dispersion techniques. AAPS PharmSciTech. 2019;1:20(5).
33. Ng HM, Saidi NM, Omar FS, Ramesh K, Ramesh S, Bashir S. Thermogravimetric analysis of polymers. In: Encyclopedia of polymer science and technology: John Wiley & Sons, Inc; 2018. p. 1–29.
34. Singh P, Kaur N, Kaur R. Perylene diimide-based pseudo-crown ether I: supramolecular aggregates for sensing of Pb2+ and diethanolamine. ChemistrySelect. 2021;6(32):8365–74.

35. Garala K, Joshi P, Patel J, Ramkishan A, Shah M. Formulation and evaluation of periodontal in situ gel. Int J Pharm Investig. 2013;3(1):29.
36. Rébufa C, Girard F, Artaud J, Dupuy N. Discrimination by infrared spectroscopy: application to micronized locust bean and guar gums. In: Modern spectroscopic techniques and applications: IntechOpen; 2020.
37. Patel M, Tekade A, Gattani S, Surana S. Solubility enhancement of lovastatin by modified locust bean gum using solid dispersion techniques. AAPS PharmSciTech. 2008;9(4):1262–9.
38. Shoormeij Z, Taheri A, Homayouni A. Preparation and physicochemical characterization of meloxicam orally fast disintegration tablet using its solid dispersion. Braz J Pharm Sci. 2017;53(4).
39. Chen Y, Chen H, Wang S, Liu C, Qian F. A single hydrogen to fluorine substitution reverses the trend of surface composition enrichment of sorafenib amorphous solid dispersion upon moisture exposure. Pharm Res. 2019;36(7).
40. Aitipamula S, Vangala VR. X-Ray crystallography and its role in understanding the physicochemical properties of pharmaceutical cocrystals. In: Journal of the Indian Institute of Science. Springer International Publishing; 2017. p. 227–243.
41. Eaton P, Quaresma P, Soares C, Neves C, de Almeida MP, Pereira E, et al. A direct comparison of experimental methods to measure dimensions of synthetic nanoparticles. Ultramicroscopy. 2017;182:179–90.
42. Alshehri S, Imam SS, Altamimi MA, Hussain A, Shakeel F, Elzayat E, et al. Enhanced dissolution of luteolin by solid dispersion prepared by different methods: physicochemical characterization and antioxidant activity. ACS Omega. 2020;5(12):6461–71.
43. Kaur L, Singh K, Paul S, Singh S, Singh S, Jain SK. A mechanistic study to determine the structural similarities between artificial membrane Strat-M^{TM} and biological membranes and its application to carry out skin permeation study of amphotericin B nanoformulations. AAPS PharmSciTech. 2018;19(4):1606–24.
44. Kaur A, Singh H, Singh Kang T, Singh S. Sustainable preparation of Fe(OH)3 and α-Fe2O3 nanoparticles employing Acacia Catechu extract for efficient removal of chromium (VI) from aqueous solution. Environmental Nanotechnology, Monitoring & Management [Internet]. 2021 Oct;100593. Available from: https://linkinghub.elsevier.com/retrieve/pii/S2215153221001689
45. Vasile A, Ignat M, Zaltariov MF, Sacarescu L, Stoleriu I, Draganescu D, et al. Development of new bexarotene-loaded mesoporous silica systems for topical pharmaceutical formulations. Acta Chim Slov. 2018;65(1):97–107.
46. Bachhav YG, Patravale VB. SMEDDS of glyburide: formulation, in vitro evaluation, and stability studies. AAPS PharmSciTech. 2009;10(2):482–7.
47. Laitinen R, Suihko E, Bjorkqvist M, Riikonen J, Lehto VP, Jarvinen K, et al. Perphenazine solid dispersions for orally fast-disintegrating tablets: physical stability and formulation. Drug Dev Ind Pharm. 2010;36(5):601–13.
48. Wikipedia contributors. Bexarotene. In: Wikipedia, the free encyclopedia [Internet]. 2022 [cited 2022 Mar 30]. Available from: https://en.wikipedia.org/w/index.php?title=Special:CiteThisPage&page=Bexarotene&id=1056047826&wpFormIdentifier=titleform
49. Rathi A, Gurudatta S, Prasarak S, Narkhede MB. An overview on the mechanisms of solubility and dissolution rate enhancement in solid dispersion [Internet]. Article in International Journal of PharmTech Research. 2013. Available from: https://www.researchgate.net/publication/286562482
50. Dionísio M, Grenha A. Locust bean gum: exploring its potential for biopharmaceutical applications. J Pharm Bioallied Sci. 2012;4(3):175–85.
51. Beneke CE, Viljoen AM, Hamman JH. Polymeric plant-derived excipients in drug delivery. Molecules. 2009;14(7):2602–20.
52. Rinaudo M. Main properties and current applications of some polysaccharides as biomaterials. Polym Int. 2008;57(3):397–430.
53. Manjoosha Srivastava by, Kapoor VP, Divisions P. Seed galactomannans: an overview. Chem Biodivers. 2005;2:295–317.
54. Kök MS. Rheological study of galactomannan depolymerisation at elevated temperatures: effect of varying pH and addition of antioxidants. Carbohydr Polym. 2010;81(3):567–71.
55. Daas PJH, Schols HA, de Jongh HHJ. On the galactosyl distribution of commercial galactomannans. Carbohydr Res [Internet]. 2000;329:609–19 Available from: www.elsevier.nl/locate/carres.
56. Potier M, Tea L, Benyahia L, Nicolaï T, Renou F. Viscosity of aqueous polysaccharide solutions and selected homogeneous binary mixtures. Macromolecules [Internet]. 2020;53(23):10514–25 Available from: https://hal.archives-ouvertes.fr/hal-03024954.
57. Sayko R, Jacobs M, Dobrynin A v. Quantifying properties of polysaccharide solutions. ACS Polymers Au 2021;1(3):196–205.
58. Kök MS, Hill SE, Mitchell JR. Viscosity of galactomannans during high temperature processing: influence of degradation and solubilisation. Food Hydrocoll [Internet]. 1999;13:535–42 Available from: www.elsevier.com/locate/foodhyd.
59. Li T, Liu R, Zhang C, Meng F, Wang L. Developing a green film from locust bean gum/carboxycellulose nanocrystal for fruit preservation. Future Foods. 2021;1:4.
60. Martins JT, Bourbon AI, Pinheiro AC, Souza BWS, Cerqueira MA, Vicente AA. Biocomposite films based on κ-carrageenan/locust bean gum blends and clays: physical and antimicrobial properties. Food Bioprocess Technol. 2013;6(8):2081–92.
61. Nanaki S, Eleftheriou RM, Barmpalexis P, Kostoglou M, Karavas E, Bikiaris D. Evaluation of dissolution enhancement of aprepitant drug in ternary pharmaceutical solid dispersions with soluplus ® and poloxamer 188 prepared by melt mixing. Sci [Internet]. 2019;1(48). Available from: www.mdpi.com/journal/sci
62. Bashardoust N, Josephine Leno Jenita J, Zakeri-Milani P. Physicochemical characterization and dissolution study of ibuprofen compression-coated tablets using locust bean gum. Dissolution Technol 2013;20(1):38–43.
63. Venkatesh N, Kuppusamy G, Nagasamy Venkatesh D, Indiran G, Reddy NS, Gowthamarajan K, et al. Design, development and evaluation of trimetazidine dihydrochloride sustained release matrix tablets. Article in International Journal of Research in Pharmaceutical Sciences [Internet]. 2011;2(2):244–251. Available from: https://www.researchgate.net/publication/268376430
64. Chen J, Qiu L, Hu M, Jin Y, Han J. Preparation, characterization and in vitro evaluation of solid dispersions containing docetaxel. Drug Dev Ind Pharm. 2008;34(6):588–94.
65. Nagpal M, Aggarwal G. Solid dispersion tablets of loratadine using locust bean gum and skimmed milk-A comparative study. Pharm Lett [Internet]. 2016;8(6):43–53 Available from: https://www.researchgate.net/publication/303973861.
66. Qi L, Guo Y, Luan J, Zhang D, Zhao Z, Luan Y. Folate-modified bexarotene-loaded bovine serum albumin nanoparticles as a promising tumor-targeting delivery system. J Mater Chem B. 2014;2(47):8361–71.
67. Xie Y, Li G, Yuan X, Cai Z, Rong R. Preparation and in vitro evaluation of solid dispersions of total flavones of Hippophae rhamnoides L. AAPS PharmSciTech. 2009;10(2):631–40.
68. Sharma A, Prakash Jain C, Singh TY. Preparation and characterization of solid dispersion of carvedilol with poloxamer 188. J Chil Chem Soc. 2013;58:1553–7.
69. Li J, Miao X, Chen T, Ouyang D, Zheng Y. Preparation and characterization of pelletized solid dispersion of resveratrol with mesoporous silica microparticles to improve dissolution by fluid-bed coating techniques. Asian J Pharm Sci. 2016;11(4):528–35.
70. Planinšek O, Kovačič B, Vrečer F. Carvedilol dissolution improvement by preparation of solid dispersions with porous silica. Int J Pharm. 2011;406(1–2):41–8.

71. van Drooge DJ, Hinrichs WLJ, Dickhoff BHJ, Elli MNA, Visser MR, Zijlstra GS, et al. Spray freeze drying to produce a stable Δ9- tetrahydrocannabinol containing inulin-based solid dispersion powder suitable for inhalation. Eur J Pharm Sci. 2005;26(2):231–40.
72. Trenfield SJ, Januskaite P, Goyanes A, Wilsdon D, Rowland M, Gaisford S, et al. Prediction of solid-state form of SLS 3D printed medicines using NIR and raman spectroscopy. Pharmaceutics [Internet]. 2022 Mar 8;14(3):589. Available from: https://www.mdpi.com/1999-4923/14/3/589
73. Andreadis II, Gioumouxouzis CI, Eleftheriadis GK, Fatouros DG. The advent of a new era in digital healthcare: a role for 3D printing technologies in drug manufacturing? Pharmaceutics [Internet]. 2022 Mar 10;14(3):609. Available from: https://www.mdpi.com/1999-4923/14/3/609
74. Fonseca-García A, Caicedo C, Jiménez-Regalado EJ, Morales G, Aguirre-Loredo RY. Effects of poloxamer content and storage time of biodegradable starch-chitosan films on its thermal, structural, mechanical, and morphological properties. Polymers (Basel). 2021;13(14).

Publisher's Note Springer Nature remains neutral with regard to jurisdictional claims in published maps and institutional affiliations.